frontiers in Physics

ORIGINAL RESEARCH
published: 22 March 2022
doi: 10.3389/fphy.2022.838124

Spatial Manipulation *via* Four-Wave Mixing in Five-Level Cold Atoms

Shoufei Gan *

School of Information Engineering, Suzhou University, Suzhou, China

In a recent publication [S. Gan, Laser Phys. 31, 055401 (2021)], a scheme for controlling the vortex four-wave mixing (FWM) in a five-level atomic system has been put forward. Based on this work, we propose a new scheme for the spatial manipulation via four-wave mixing in a five-level atomic system when the radial index is considered. It is found that the phase and intensity of the FWM field can be spatially manipulated. More importantly, we show the superposition modes created by the interference between the FWM field and a same-frequency Gaussian beam, which can also be controlled *via* the corresponding parameters. Our research is helpful to understand and manipulate optical vortices and can be widely used in quantum computation and communication.

Keywords: four-wave mixing, cold atoms, optical vortices, orbital angular momentum, Laguerre-Gaussian beam

OPEN ACCESS

Edited by:
Weibin Li,
University of Nottingham,
United Kingdom

Reviewed by:
Zhiping Wang,
Anhui University, China
Liping Li,
Zhongyuan University of Technology,
China

***Correspondence:**
Shoufei Gan
ganshfei@163.com

Specialty section:
This article was submitted to Quantum Engineering and Technology, a section of the journal Frontiers in Physics

Received: *17 December 2021*
Accepted: *21 February 2022*
Published: *22 March 2022*

Citation:
Gan S (2022) Spatial Manipulation via Four-Wave Mixing in Five-Level Cold Atoms. Front. Phys. 10:838124. doi: 10.3389/fphy.2022.838124

1 INTRODUCTION

The Laguerre–Gaussian (LG) light carrying orbital angular momentum (OAM) [1] has attracted a lot of interest due to its unique amplitude and phase structures. In particular, the four-wave mixing (FWM) based on OAM light has emerged as a hot topic in recent years. For instance, Qiu et al. proposed a scheme to demonstrate the manipulation of space-dependent four-wave mixing (FWM) in a four-level atomic system [2]. By adjusting the detuning of the control field, one can effectively control the FWM output field. Yu et al. described a theoretical investigation of a FWM scheme in a six-level atomic system driven by a field with OAM and making use of two electromagnetically induced transparency (EIT) control fields [3]. The obtained results allow one to control the helical phase of the output FWM field by varying the intensities of the two EIT control fields as well as the detuning of the probe field. Quite recently, Wang et al. have also proposed some schemes to control vortex FWM carrying OAM in different nanostructures [4–6].

In this paper, we investigated the spatial manipulation *via* four-wave mixing in a five-level atomic system. Quite recently, we have proposed a scheme for modulating the spatial vortex FWM in a five-level atomic system [7]. However, different from this previous study, the major features of applying our considered scheme are as follows. First, the main difference between our scheme and the one in [7] is that we have shaped the LG field as a double-ring LG mode with the radial index $p = 1$ while in [7] the radial index is 0. This scheme has many advantages for controlling the FWM in comparison with the publication [7]. For example, the double-ring LG mode provides two FWM channels, and in different channels the spatial variation of the FWM are different. Second, in this scheme more physical parameters (e.g., the radial index $p = 1$) can be manipulated and hence one can select suitable radial index p to explore singularity characteristics of helical phase wavefront in nonlinear processes. Third, we display the superposition modes created by the interference between the FWM field and a same-frequency Gaussian beam, which show a more flexible intensity control or phase control for the superposition modes.

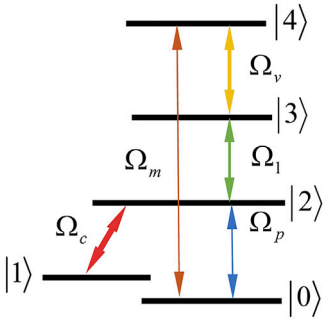

FIGURE 1 | Schematic of a five-level atomic system.

2 THEORETICAL MODEL AND EQUATIONS

We consider an atomic system as shown in **Figure 1**. A probe field with Rabi frequency $\Omega_p = \Omega_{p0}e^{-(r/R_p)^2}\sqrt{\pi/(2\ln 2)}\exp[-t^2/(2\ln 2/\pi^2)]$ (Ω_{p0} and R_p are the amplitude and transverse radius with t being the time) is applied to the transition $|2\rangle \leftrightarrow|0\rangle$. A control field with Rabi frequency Ω_c drives the transition $|2\rangle \leftrightarrow|1\rangle$. A pump field with Rabi frequency Ω_1 drives the transition $|3\rangle \leftrightarrow|2\rangle$, while a LG field with Rabi frequency Ω_v drives the transition $|4\rangle \leftrightarrow|3\rangle$. Here Ω_v is defined as

$$\Omega_v = \Omega_{v0}\Omega(r)e^{-il\phi}, \tag{1}$$

where $\Omega(r) = \frac{\sqrt{2p!/\pi(p+|l|)!}}{\omega_0}(\frac{\sqrt{2}r}{\omega_0})^{|l|}L_p^{|l|}(\frac{2r^2}{\omega_0^2})e^{-r^2/\omega_0^2}$, Ω_{v0} is the initial Rabi frequency, r is the radius and the beam waist is ω_0. ϕ is the azimuthal angle and $L_p^{|l|}$ is the Laguerre polynomial. The radial index and azimuthal index are defined by p and l, respectively.

Making use of the Schrödinger equation, the dynamical equations for the atomic probability amplitudes $A_j(j = 1–4)$ in the interaction picture are given by [8].

$$\dot{A}_1 = \left[i\left(\Delta_p - \Delta_c\right) - \gamma_1\right]A_1 + i\Omega_c^* A_2, \tag{2a}$$

$$\dot{A}_2 = i\Omega_p A_0 + \left(i\Delta_p - \gamma_2\right)A_2 + i\Omega_c A_1 + i\Omega_1^* A_3, \tag{2b}$$

$$\dot{A}_3 = i\Omega_1 A_2 + i\Omega_v^* e^{i\delta\vec{k}\cdot\vec{r}}A_4 + \left[i\left(\Delta_p + \Delta_3\right) - \gamma_3\right]A_3, \tag{2c}$$

$$\dot{A}_4 = i\Omega_m A_0 + i\Omega_v e^{-i\delta\vec{k}\cdot\vec{r}}A_3 + \left[i\left(\Delta_p + \Delta_3 + \Delta_4\right) - \gamma_4\right]A_4, \tag{2d}$$

where Δ_p, Δ_c, Δ_3 and Δ_4 are the detunings of the fields. The $\delta\vec{k} = \vec{k}_m - (\vec{k}_p + \vec{k}_1 + \vec{k}_v)$ is phase mis-matching condition, and $\vec{k}_i\,(i = p, 1, v, m)$ are the wave vectors of the corresponding fields. The γ_n $(n = 1–4)$ are decay rates.

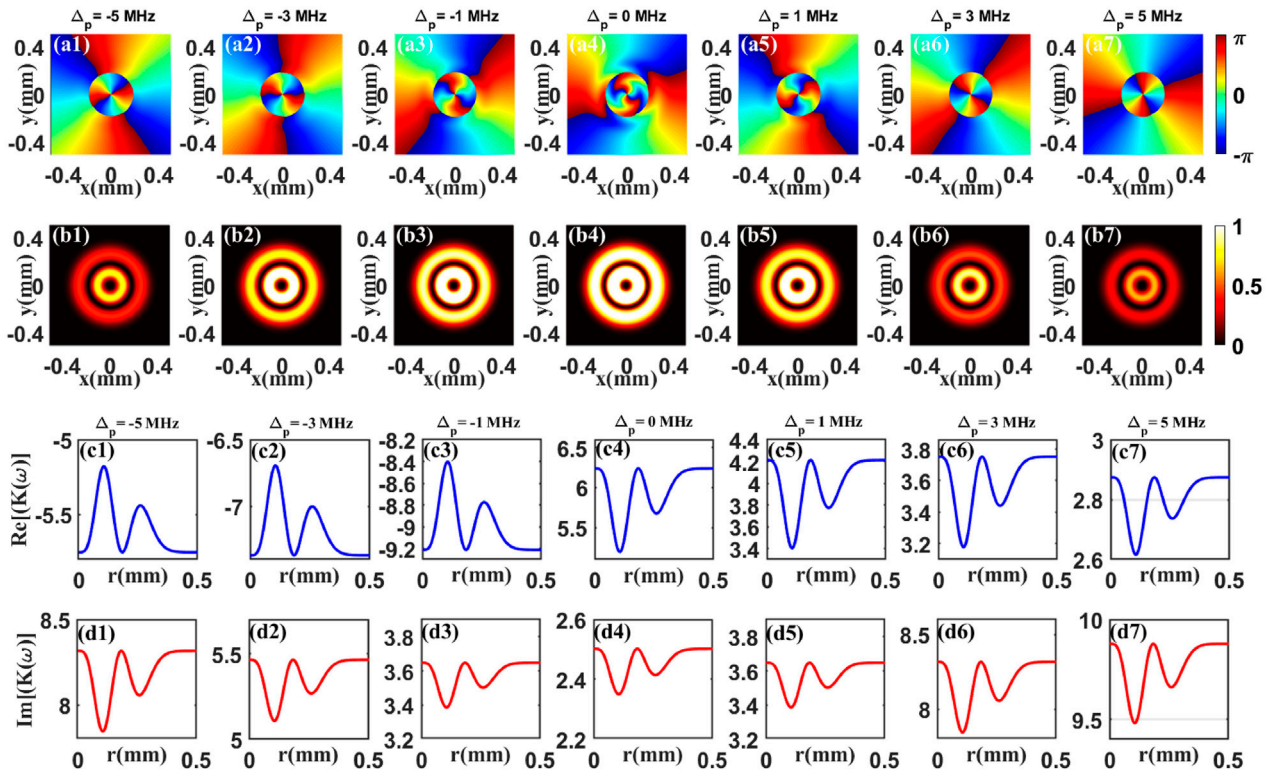

FIGURE 2 | Phase **(A1–A7)** and normalized intensity **(B1–B7)** patterns of the FWM field for different probe detuning Δ_p. The real **(C1–C7)** and imaginary **(D1–D7)** parts of dispersion relation $K(\omega)$ versus radius r for different probe detuning Δ_p. The other parameters are $\omega_0 = 0.18$ mm, $R_p = 3\omega_0$, $\omega = 3$ MHz, $z = 15$ mm, $p = 1$, $l = 2$, $\gamma_1 = 1 \times 10^{-4}$ MHz, $\gamma_2 = 6$ MHz, $\gamma_3 = 0.66$ MHz, $\gamma_4 = 0.08$ MHz, $\Omega_1 = 12$ MHz, $\Omega_{v0} = 2.5$ MHz, $\Omega_c = 5.5$ MHz, $\Omega_{p0} = 0.55$ MHz, $\Delta_c = \Delta_3 = \Delta_4 = 0$, $\kappa_{02} = 200$ MHz/mm, $\kappa_{04} = 0.01\kappa_{02}$.

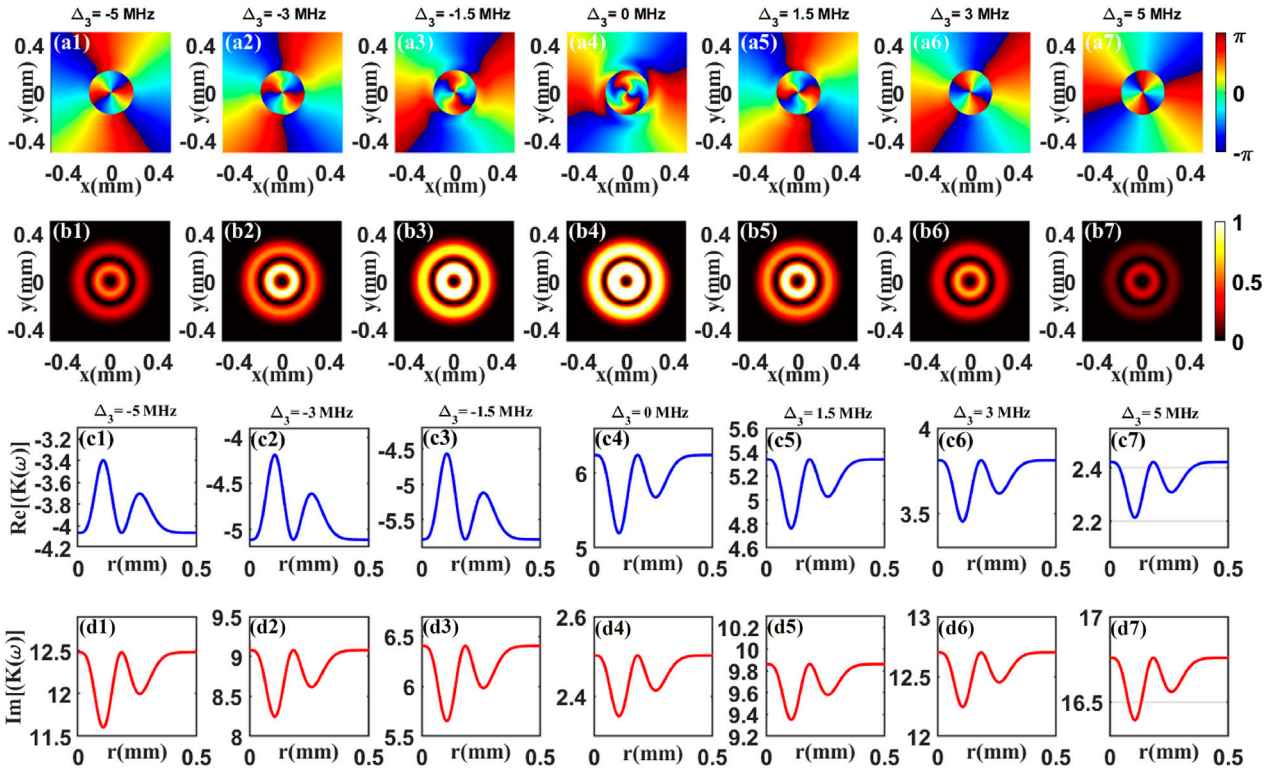

FIGURE 3 | Phase **(A1–A7)** and normalized intensity **(B1–B7)** patterns of the FWM field for different detuning Δ_3. The real **(C1–C7)** and imaginary **(D1–D7)** parts of dispersion relation $K(\omega)$ versus radius r for different detuning Δ_3. The other parameters are the same as in **Figure 2**.

Under the slowly varying envelope approximation, the propagation equations of the probe and FWM fields are governed by the Maxwell equations

$$\frac{\partial \Omega_{p(m)}}{\partial z} + \frac{\partial \Omega_{p(m)}}{c\partial t} = \frac{i}{2k_{p(m)}}\nabla_{\perp}^{2}\Omega_{p(m)} + i\kappa_{02(04)}aA_{2(4)}A_{0}^{*}, \quad (3)$$

where $k_{p(m)}$ is the wave number of the probe field (FWM field). $\kappa_{02(04)} = 2N\omega_{p(m)}|D_{02(04)}|^2/(c\hbar)$ is the propagation constant, which is related to the frequently used oscillator strengths of the transition $|0\rangle \leftrightarrow |2\rangle$ ($|4\rangle$). N and $D_{02(04)}$ are the atomic density and dipole moment between states $|0\rangle$ and $|2\rangle$ ($|4\rangle$), respectively.

We assume all the atoms are in the ground state $|0\rangle$ i.e. $|A_0|^2 \approx 1$ and use the condition of phase matching $\delta\vec{k} = 0$. By applying Fourier transformations $A_j(t) = \int \tilde{A}_j(\omega)e^{-i\omega t}d\omega$ ($j = 1-4$) to Eqs 2a, 3 and obtain [9].

$$f_1\tilde{A}_1 + \Omega_c^*\tilde{A}_2 = 0, \quad (4a)$$

$$\Omega_c\tilde{A}_1 + f_2\tilde{A}_2 + \Omega_1^*\tilde{A}_3 = -\tilde{\Omega}_p, \quad (4b)$$

$$\Omega_1\tilde{A}_2 + f_3\tilde{A}_3 + \Omega_v^*\tilde{A}_4 = 0, \quad (4c)$$

$$\Omega_v\tilde{A}_3 + f_4\tilde{A}_4 = -\tilde{\Omega}_m, \quad (4d)$$

and the Maxwell's equations $\Omega_{p(m)}$ obeyed as follows

$$\frac{\partial \tilde{\Omega}_{p(m)}}{\partial z} - \frac{i\omega}{c}\tilde{\Omega}_{p(m)} = \frac{i}{2k_{p(m)}}\nabla_{\perp}^{2}\tilde{\Omega}_{p(m)} + i\kappa_{02(04)}\tilde{A}_{2(4)}, \quad (5)$$

where ω is the Fourier frequency. $f_1 = \omega + \Delta_p - \Delta_c + i\gamma_1, f_2 = \omega + \Delta_p + i\gamma_2, f_3 = \omega + \Delta_p + \Delta_3 + i\gamma_3, f_4 = \omega + \Delta_p + \Delta_3 + \Delta_4 + i\gamma_4$, and $\tilde{\Omega}_{p(m)}$ are the Fourier transformations of $\Omega_{p(m)}$. The first terms on the right-hand sides of the **Eq. 5** accounts for light diffraction. Light diffraction can be neglected if the propagation distance is much smaller than the Rayleigh ranges of the probe pulse or the generated FWM field [10, 11], i.e. $\pi\omega_0^2/\lambda \gg L$. We take the propagation distance z = 15 mm, the transverse characteristic dimension $w_T = \omega_0$ = 0.18 mm and the wavelength of the FWM field $\lambda \approx$ 300 nm, obtaining $\pi\omega_0^2/\lambda \approx$ 339.12 mm $\gg$ 15 mm. So it is safe to ignore diffraction in this work.

Using the initial condition $\tilde{\Omega}_m(z = 0, \omega) = 0$, the generated FWM field is given by

$$\tilde{\Omega}_m(z,\omega) = \frac{\tilde{\Omega}_p(z = 0,\omega)\kappa_{04}\beta_1\Omega_1\Omega_v}{M[K_+(\omega) - K_-(\omega)]}\left(e^{iK_-(\omega)z} - e^{iK_+(\omega)z}\right), \quad (6)$$

where $K_{\pm}(\omega) = \frac{\omega}{c} + \frac{F_p+F_m}{2} \pm \sqrt{[\frac{F_p-F_m}{2}]^2 + G}$, $F_p = -(f_3f_4 - |\Omega_v|^2)f_1\kappa_{02}/M$, $F_m = -[M + (f_1f_2 - |\Omega_c|^2)|\Omega_v|^2]\kappa_{04}/Mf_4$, $G = f_1^2|\Omega_1|^2|\Omega_v|^2\kappa_{02}\kappa_{04}/M^2$, $M = (f_1f_2 - |\Omega_c|^2)(f_3f_4 - |\Omega_v|^2) - |\Omega_1|^2f_1f_4$, with $\tilde{\Omega}_p(z = 0, \omega) = \Omega_{p0}e^{-(r/\omega_{p0})^2}\exp[-\omega^2/(2\pi^2/\ln 2)]$. We can see that there exist two modes $K_+(\omega)$ and $K_-(\omega)$ described by the dispersion relation $K(\omega) = K_+(\omega) + K_-(\omega)$ in **Eq. 6**, the real part Re$[K(\omega)]$ reflects the phase while the imaginary part Im $[K(\omega)]$ represents the absorption [12].

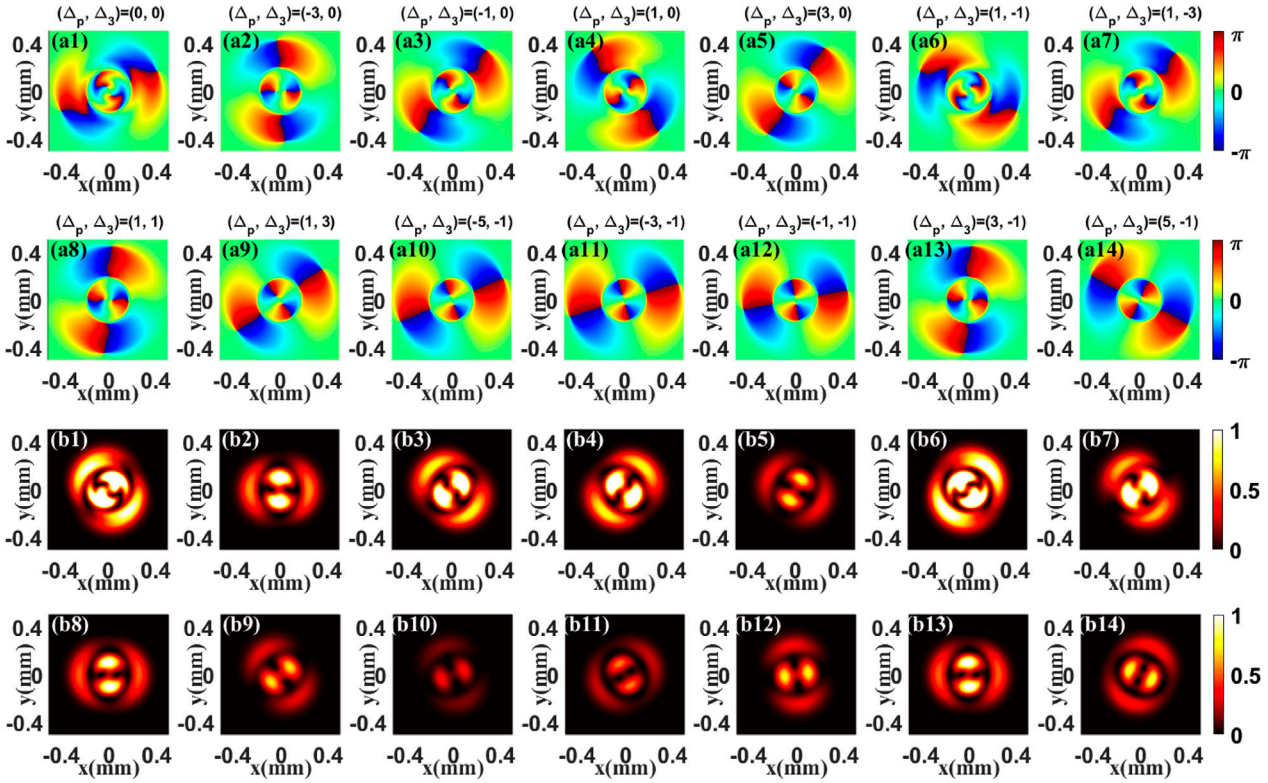

FIGURE 4 | Superposition phase **(A1–A14)** and intensity **(B1–B14)** patterns of FWM field and the same-frequency Gaussian beam $\Omega_G = e^{-(r/2\omega_0)^2}$ for different Δ_p and Δ_3. The other parameters are the same as in **Figure 2**.

3 RESULTS AND DISCUSSION

In this section, we aim to study the effects of the different parameters on phase and intensity of the FWM field $\tilde{\Omega}_m(z,\omega)$. In order to clearly show the spatial-dependent mechanism, the superposition modes created by the interference between the FWM field and a same-frequency Gaussian beam are also provided.

In **Figure 2**, we plot the phase and the normalized intensity patterns of the FWM field versus the (x, y) for different probe detuning Δ_p. As we expected, both the phase (**Figures 2A1–A7**) and intensity (**Figures 2B1–B7**) patterns are divided into two parts. From this figure, one can find that, upon increasing Δ_p from 1 MHz to ±5 MHz, the value of intensity decrease progressively while the phase twist is suppressed. The key factor is that the azimuthal dependent absorption and dispersion properties of the FWM field are modulated, which lead to the corresponding results. Moreover, the real (**Figures 2C1–C7**) part and imaginary (**Figures 2D1–D7**) part of dispersion relation $K(\omega)$ are shown in **Figure 2**, which have given the physical reason for the phase and the intensity patterns of the FWM field being changed in **Figure 2**.

In **Figure 3**, we present the phase and the normalized intensity patterns of the FWM field for different detuning Δ_3. By direct comparison in **Figures 2**, **3**, we obtain that the situation in **Figure 3** is nearly the same as the **Figure 2**. Such results indicate that the OAM phase is transferred to the FWM field and is modulated *via* detuning Δ_3. Here, we also provide the real part and imaginary part of dispersion relation in **Figures 3C1–C7** and **Figures 3D1–D7**. By increasing the detuning Δ_3, both the imaginary part and real part are changing. So we can see the varying phase and intensity of the FWM field.

Next, to obtain a better understanding of the vortex modulation, we show the superposition patterns of the FWM field and a same-frequency Gaussian beam in **Figure 4**. As illustrated in **Figure 4**, the superposition patterns are extremely rotated for different detunings Δ_p and Δ_3. The reason for this is that, due to the equiphase surface of Gaussian beam is a plane, azimuthally phase difference between the FWM field and Gaussian beam is very sensitive to detunings (Δ_p, Δ_3), which reflects the different superposition patterns. The findings in **Figure 4** imply that the OAM phase is indeed transferred to the FWM field and has a spatial dependency, which is originated from the spatial-sensitive absorption and dispersion properties induced by the three fields in the present system.

We note that, very recently, some theoretical schemes for controlling the space-dependent FWM in atoms [2, 3] or in semiconductor quantum wells [4–6] have been proposed. Comparing with those schemes, the major features of our proposal are the following. First, we have utilized the EIT induced by a additional control beam Ω_c. The EIT scheme has

many advantages for controlling the FWM in comparison with the one in [2]. For example, the coherent optical FWM with the EIT condition mediated by detunings Δ_p or Δ_3 will lead to many orders of magnitude enhancement in the amplitude of the generated wave (e.g., see **Figures 2**, **3**). Second, Different from the results obtained in [3], we display the superposition modes created by the interference between the FWM field and a same-frequency Gaussian beam. It is found that the superposition modes can be spatially manipulated *via* the corresponding parameters, which show a more flexible intensity control or phase control for the superposition modes. Third, unlike in solid-state systems [4–6], nonlinear effects are highly efficient and require only low light intensities in atomic vapors, which is convenient for the experimental realization of our scheme.

Before ending this section, it is worthwhile to briefly discuss the possible experimental realization of our scheme. Such an atomic structure can be realized in cold ^{85}Rb atoms. The designated states can be chosen as: $|0\rangle = |5S_{1/2}, F = 1\rangle$, $|1\rangle = |5S_{1/2}, F = 2\rangle$, $|2\rangle = |5P_{3/2}\rangle$, $|3\rangle = |5D_{5/2}\rangle$ and $|4\rangle = |nP_{3/2}\rangle$ ($n > 10$). Three transitions are $|5S_{1/2}, F = 1\rangle \leftrightarrow |5P_{3/2}\rangle$ at 780 nm, $|5P_{3/2}\rangle \leftrightarrow |5D_{5/2}\rangle$ at 776 nm, $|5D_{5/2}\rangle \leftrightarrow |63P_{3/2}\rangle$ at 1260 nm, and a Rydberg transition generated the FWM field $|5S_{1/2}, F = 1\rangle \leftrightarrow |63P_{3/2}\rangle$ at 300 nm.

4 CONCLUSION

In summary, we have studied the spatial manipulation *via* four-wave mixing (FWM) in a five-level atomic system. Interestingly, by adjusting the detunings, one can effectively modulate the phase and intensity of the FWM field when the radial index is considered. More importantly, we show the superposition modes created by the interference between the FWM field and a same-frequency Gaussian beam, which show many interesting properties. So our results may be helpful to investigate the interactions between OAM light and quantum media [13, 14].

DATA AVAILABILITY STATEMENT

The original contributions presented in the study are included in the article/Supplementary material, further inquiries can be directed to the corresponding author.

AUTHOR CONTRIBUTIONS

The author confirms being the sole contributor of this work and has approved it for publication.

ACKNOWLEDGMENTS

This work is supported by the key project of continuing education and teaching reform of Department of Education of Anhui Province (2019jxjj39) and the key project of research and development of Anhui Province (NO. 202004a05020043).

REFERENCES

1. Allen L, Beijersbergen MW, Spreeuw RJC, Woerdman JP. Orbital Angular Momentum of Light and the Transformation of Laguerre-Gaussian Laser Modes. *Phys Rev A* (1992) 45:8185. doi:10.1103/physreva.45.8185
2. Qiu J, Wang Z, Ding D, Huang Z, Yu B. Control of Space-dependent Four-Wave Mixing in a Four-Level Atomic System. *Phys Rev A* (2020) 102:033516. doi:10.1103/physreva.102.033516
3. Yu C, Wang Z. Engineering Helical Phase via Four-Wave Mixing in the Ultraslow Propagation Regime. *Phys Rev A* (2021) 103:013518. doi:10.1103/physreva.103.013518
4. Zhang Y, Wang Z, Qiu J, Hong Y, Yu B. Spatially Dependent Four-Wave Mixing in Semiconductor Quantum wells. *Appl Phys Lett* (2019) 115:171905. doi:10.1063/1.5121275
5. Wang Z, Zhang Y, Paspalakis E, Yu B. Efficient Spatiotemporal-Vortex Four-Wave Mixing in a Semiconductor Nanostructure. *Phys Rev A* (2020) 102:063509. doi:10.1103/physreva.102.063509
6. Qiu J, Wang Z, Ding D, Li W, Yu B. Highly Efficient Vortex Four-Wave Mixing in Asymmetric Semiconductor Quantum wells. *Opt Express* (2020) 28(3):2975–86. doi:10.1364/oe.379245
7. Gan S. Spatial Vortex Four-Wave Mixing in a Five-Level Atomic System. *Laser Phys* (2021) 31:055401. doi:10.1088/1555-6611/abee8e
8. Wu Y, Payne MG, Hagley EW, Deng L. Efficient Multiwave Mixing in the Ultraslow Propagation Regime and the Role of Multiphoton Quantum Destructive Interference. *Opt Lett* (2004) 29:2294. doi:10.1364/ol.29.002294
9. Wu Y, Saldana J, Zhu Y. Large Enhancement of Four-Wave Mixing by Suppression of Photon Absorption from Electromagnetically Induced Transparency. *Phys Rev A* (2003) 67:013811. doi:10.1103/physreva.67.013811
10. Hong Y, Wang Z, Ding D, Yu B. Ultraslow Vortex Four-Wave Mixing via Multiphoton Quantum Interference. *Opt Express* (2019) 27:29863. doi:10.1364/oe.27.029863
11. Chen J, Wang Z, Yu B. Spatially Dependent Hyper-Raman Scattering in Five-Level Cold Atoms. *Opt Express* (2021) 29(7):10914–22. doi:10.1364/oe.420015
12. Wu Y, Yang X. Highly Efficient Four-Wave Mixing in Double-Λsystem in Ultraslow Propagation Regime. *Phys Rev A* (2004) 70:053818. doi:10.1103/physreva.70.053818
13. Qiu J, Wang Z, Yu B. Generation of New Structured Beams via Spatially Dependent Transparency. *Quan Inf Process* (2019) 18:1. doi:10.1007/s11128-019-2278-6
14. Zhang K, Wang W, Liu S, Pan X, Du J, Lou Y, et al. Reconfigurable Hexapartite Entanglement by Spatially Multiplexed Four-Wave Mixing Processes. *Phys Rev Lett* (2020) 124:090501. doi:10.1103/physrevlett.124.090501

Conflict of Interest: The author declares that the research was conducted in the absence of any commercial or financial relationships that could be construed as a potential conflict of interest.

Publisher's Note: All claims expressed in this article are solely those of the authors and do not necessarily represent those of their affiliated organizations, or those of the publisher, the editors and the reviewers. Any product that may be evaluated in this article, or claim that may be made by its manufacturer, is not guaranteed or endorsed by the publisher.